Synthesis of Polymeric Photoinitiators Containing Pendent Chromophore−Borate Ion Pairs: Photochemistry and Photopolymerization Activities[1]

Ananda M. Sarker, Ken Sawabe, Bernd Strehmel, Yuji Kaneko, and Douglas C. Neckers*

Center for Photochemical Sciences, Bowling Green State University, Bowling Green, Ohio 43403

Received January 28, 1999; Revised Manuscript Received May 17, 1999

ABSTRACT: Poly(methyl methacrylate)s containing light-absorbing acetonaphthone and acetobenzo[*b*]-furan as electron acceptors paired with tetraorganyl borates have been synthesized. Upon irradiation at 350 nm, oxidative carbon−nitrogen and reductive carbon−boron bond cleavage occurs, producing reactive radicals and tertiary amines. The efficiency of bond-breaking processes is found to be dependent on the nature of both the acceptors and the donors. Photoinduced polymerizations initiated by these polymeric initiators have been compared to 2,2-dimethoxy-2-phenylacetophenone (Irgacure 651) in tetraethylene glycoldiacrylate (TEGDA). Differences in the efficiency of the initation are accounted for by parameters associated with photoreactivity.

Introduction

Polymeric photoinitiators with reactive functionalities capable of coreaction have recently been of growing interest, particularly for laser-induced polymerization[2,3] and for holography.[4] Such initiators have several advantages compared to low molecular weight analogues. Photoproducts produced from small molecules during photolysis are generally trapped in the cured coating, and many induce photodegradation over time. An issue of primary concern in packaging systems is that the low molecular weight species formed from the photoinitiator may migrate from the coating into a packaged product. These complications may be avoided by the use of polymeric photoinitiators that reduce the tendency to migrate owing to their polymeric nature. The addition of polymeric photoinitiators to a formulation also increases the viscosity of the formulation, and they sometimes show improved compatibility in formulations due to the nature of the polymeric backbone and the pendent groups.[2]

We, and others, have developed photoinitiators bearing chromophore−borate ion pairs that give an active alkyl radical and a tertiary amine upon irradiation.[5−13] Formation of an alkyl radical takes place after electron transfer to the excited chromophore from the borate anion, and it is the alkyl radical that initiates acrylate polymerization.[14] The tertiary amine also plays an important role.[15] Generally, in free radical mediated polymerization, photogenerated radicals and the growing macroradicals are quenched by oxygen. As a result, the rate of polymerization is decreased and molecular weight distribution of the polymer affected. The formation of tertiary amine in polymerization processes helps to ameliorate the situation. This benefit is somehow offset if the amine is added separately to the formulation by the tendency due to form a yellowish color and volatile toxic materials. This chemistry may, in principle, be extended to polymeric systems, if properly designed.

In this paper we report a new class of polymeric systems containing chromophore−borates as the side chains. Such polymers are susceptible to 350 nm wavelength irradiation and generate polymeric tertiary amines and reactive radicals as a result of bond cleavage reactions. Their photoactivities in the photopolymerization were compared with commercial Irgacure 651. Emphasis is given to the photochemistry and the photoproducts as well as their contribution to the photoinitiation of polymerization.

Experimental Section

General. Melting point determinations were made using a Thomas-Hoover capillary melting point apparatus; all temperatures are uncorrected. All new compounds were characterized by NMR, IR, and elemental analysis (Atlantic Microlab, Inc., Georgia). Nuclear magnetic resonance (NMR) spectra were taken on a Gemini GEM-200 (200 MHz). Chemical shifts are reported in parts per million (ppm) relative to TMS at 0.0 ppm on the δ scale. ^{13}C NMR spectra were recorded on a Gemini GEM-200 (50 MHz), and chemical shifts are reported in δ units, unless otherwise mentioned. Photolysis experiments were carried out in a Rayonet model photochemical reactor fitted with mercury lamps (300−400 nm). Triethylene glycol diacrylate (TEGDA) was purchased from Sartomer and used as received. Irgacure 651 (2,2-dimethoxy-2-phenylacetophenone) was obtained from Ciba-Geigy and purified by recrystallization from methanol. Unless otherwise indicated, all reagents and solvents were obtained from Aldrich Chemical Co. and used as received.

Thermogravimetric analyses were carried out using a Du Pont TGA-951 with a thermal analyzer 2100 system. TGA samples were heated at a rate of 20 °C/min with a purified nitrogen gas flow of 20 cm^3/min. Phase transition temperatures were measured with a Perkin-Elmer differential scanning calorimeter (DSC-2) calibrated with indium and tin, under a flow of nitrogen with the heating and cooling rates of 20 °C/min. Polymer samples weighing 5−10 mg were used for this analysis. The melting temperature, T_m, was taken as the onset of the transitions in either the first or second heating cycle, whichever was more prominent.

Photoinitiation efficiency measurements were carried out on a CM-1000 cure monitor at Spectra Group Ltd., Inc. Solutions of each polymeric initiator in TEGDA containing 0.05 wt % of DASB (5-(dimethylamino)naphthalene-1-sulfonyl-*n*-butylamide) were prepared. The concentration of the initiators in each of the solution was maintained at 0.1 wt %, and absorbance of the photoinitiator was measured at 350 nm. A

10.1021/ma990127c CCC: $18.00
Published on Web 07/13/1999

precisely 0.175 mm thick layer of each of the solution was prepared by squeezing a drop of the mixture between two glass slides separated by the appropriate spacers. A small spot on this thin layer was cured with the excitation beam of the CM-1000, and the polymerization process was simultaneously monitored from the change of the fluorescence spectrum of the incorporated probe, which in turn was indicated by the ratio of the fluorescence intensity at two wavelengths (456 and 558 nm) on each side of the emission maximum. The excitation of both the initiator and the probe was accomplished by the monochromic excitation beam of CM-1000 set at 350 nm. All kinetic measurements were obtained under steady-state conditions, and the relative efficiency of the initiators was calculated as described earlier.[16] The optical density of the photoinitiators was measured at 350 nm.

Quantum Yield Determination. All samples were irradiated in the same solvent in quartz cuvetts at 340 nm while being stirred. The light emitted from a 200 W high-pressure mercury lamp was used as light source. A filter combination consisting of cutoff filter (transmittance between 300 and 500 nm) and interference filter centered at 340 nm was used to get the desired wavelength with a half-width of 10 nm at this wavelength. After passing of that optical combination and a time controlled shutter, the light was focused on the sample. Acridine actinometry (3×10^{-4} M, $\Phi_d = 0.032$, $\lambda_{ex} = 340$ nm) was applied to get the quantity for the light intensity in photons/time.[17] The extent of reaction was measured by steady-state UV absorption spectroscopy. Quantum yields were determined from the initial 10% conversions using the equation described previously.[18] The optical density of all solutions was adjusted at an appropriate value at the beginning of the photolysis. In the case of anaerobic irradiation conditions, solutions of **7**−**8** dissolved in acetonetrile were purged with argon.

***N,N*-Dimethyl-*N*-(2-acetylnaphthone)-*N*-(2-methacryloylethyl)ammonium Bromide (6a).** To a solution of 2-bromoacetylnaphthone (5.54 g, 22.24 mmol) in 60 mL of chloroform:ether (1:1) was added 2-(dimethylamino)ethyl methacrylate (3.90 g, 24.80 mmol) dropwise with stirring at room temperature. The solution was stirred for 4 h. The thick white precipitate was separated by filtration and washed thoroughly with ether. After recrystallization from acetone−methanol mixture, **6a** was obtained as white crystals (8.28 g, 92% yield); mp 153−154 °C. ^{1}H NMR (CD_3OD, δ): 8.69 (s, 1H), 8.03 (m, 4H), 7.68 (m, 2H), 5.87 (s, 1H), 5.36 (s, 1H), 4.90 (s, 2H), 4.86 (m, 2H), 4.29 (m, 2H), 3.54 (s, 6H), 1.74 (s, 3H). ^{13}C NMR (CD_3OD, δ): 191.94, 167.60, 137.51, 136.53, 133.60, 132.80, 132.00, 130.94, 130.63, 129.91, 128.90, 128.38, 127.18, 123.90, 64.25, 59.52, 59.47, 53.93, 18.27. Anal. Calcd for $C_{20}H_{24}BrNO_3$: C, 59.15; H, 5.91; N, 3.45; Br, 19.68. Found: C, 59.03; H, 5.88; N, 3.46; Br, 19.76.

***N,N*-Dimethyl-*N*-(2-acetylbenzo[*b*]furan)-*N*-(2-methacryloylethyl)ammonium Bromide (6b).** Analogous to the procedure described above, 2-bromoacetylbenzo[*b*]furan (3.05 g, 12.75 mmol)[19] and 2-(dimethylamino)ethyl methacrylate (6.0 g, 38.16 mmol) were allowed to react in diethyl ether, followed by recrystallization from ethyl acetate−methanol to provide **6b** as white crystals (3.17 g, 63%); mp 163−164 °C. ^{1}H NMR (CD_3OD, δ): 7.78 (m, 2H), 7.52 (m, 2H), 7.31 (m, 1H), 5.83 (s, 1H), 5.32 (s, 1H), 4.80 (s, 2H), 4.57 (m, 2H), 4.06 (m, 2H), 3.40 (s, 6H), 1.71 (s, 3H). ^{13}C NMR (CD_3OD, δ): 184.13, 169.41, 159.11, 153.22, 138.57, 132.67, 129.85, 128.87, 127.58, 126.96, 118.70, 115.13, 66.58, 61.27, 61.30, 55.75, 20.10. Anal.Calcd for $C_{18}H_{22}BrNO_4$: C, 54.58; H, 5.55; N, 3.53; Br, 20.17. Found: C, 54.43; H, 5.53; N, 3.50; Br, 20.28.

***N,N*-Dimethyl-*N*-(2-acetylnaphthone)-*N*-(2-methacryloylethyl)ammonium Tetraphenylborate (3a).** To a solution of **6a** (2.27 g, 5.60 mmol) in water (75 mL) and methanol (8 mL) was added slowly an aqueous sodium salt of tetraphenylborate (1.95 g, 5.70 mmol) with stirring at room temperature. A slight stoichiometric excess of sodium salt of tetraphenylborate was used to ensure complete conversion. A white solid gradually precipitated, and the resulting mixture was stirred an additional 30 min. The solid was filtered, washed with water, and then air-dried overnight. After recrystallization from ethanol, **3a** was obtained as white solid (2.28 g, 63%); mp 171−172 °C. ^{1}H NMR (acetone, δ): 8.71 (s, 1H), 8.06 (m, 4H), 7.72 (m, 2H), 7.38 (m, 8H, ortho to B), 6.93 (t, $J = 7.2$ Hz, 8H, meta to B), 6.78 (m, 4H, para to B), 5.95 (s, 1H), 5.68 (s, 1H), 5.50 (m, 2H), 4.78 (m, 2H), 4.38 (m, 2H), 3.70 (s, 6H), 1.78 (s, 3H). Anal. Calcd for $C_{44}H_{44}BNO_3$: C, 81.90; H, 6.82; N, 2.17. Found: C, 81.72; H, 6.88; N, 2.15.

***N,N*-Dimethyl-*N*-(2-acetylbenzo[*b*]furan)-*N*-(2-methacryloylethyl)ammonium Tetraphenylborate (3b).** As in the procedure described for **3a**, an aqueous sodium salt of tetraphenylborate (2.50 g, 10.25 mmol) and **6b** (2.61 g, 6.58 mmol) in water were allowed to react, followed by recrystallization from ethyl acetate−acetonitrile mixture to give **3b** as white powder (2.83 g, 68%); mp 97−98 °C. ^{1}H NMR (CD_3CN, δ): 7.85 (d, $J = 7.8$ Hz, 1H), 7.78 (s, 1H), 7.63 (d, $J = 3.6$ Hz, 2H), 7.42 (m, 1H), 7.28 (m, 8H, ortho to B), 6.99 (t, $J = 7.4$ Hz, 8H, meta to B), 6.84 (t, $J = 7.4$ Hz, 4H, para to B), 5.93 (s, 1H), 5.49 (s, 1H), 4.87 (s, 2H), 4.51 (m, 2H), 3.96 (m, 2H), 3.31 (s, 6H), 1.80 (s, 3H). Anal. Calcd for $C_{42}H_{42}BNO_4$: C, 79.41; H, 6.61; N, 2.20. Found: C, 79.29; H, 6.65; N, 2.19.

***N,N*-Dimethyl-*N*-(2-acetylnaphthone)-*N*-(2-methacryloylethyl)ammonium Triphenylbutylborate (4a).** To a solution of **6a** (1.85 g, 4.55 mmol) in 50 mL of water−methanol (5:1) mixture was added dropwise lithium salt of triphenylbutyl borate (1.50 g, 4.90 mmol) in minimum water with stirring at room temperature. After 30 min, water (300 mL) was added, and the solution was stirred for another 30 min. The white solid was separated by filtration and washed thoroughly with water. After air-dried, it was recrystallized from ethanol−acetone mixture and vacuum-dried. The monomer **4a** was obtained as a white powder (1,05 g, 38%); mp 165−66 °C. ^{1}H NMR (CD_3CN, δ): 8.55 (s, 1H), 8.02 (m, 4H), 7.71 (m, 2H), 7.28 (m, 6H, ortho to B), 6.96 (m, 6H, meta to B), 6.81 (m, 3H, para to B), 5.87 (s, 1H), 5.42 (s, 1H), 5.08 (s, 2H), 4.53 (m, 2H), 4.02 (m, 2H), 3.36 (s, 6H), 2.19 (m, 2H), 1.21 (m, 2H), 0.91 (m, 2H), 0.80 (m, 3H). Anal. Calcd for $C_{42}H_{48}BNO_3$: C, 80.68; H, 7.68; N, 2.24. Found: C, 80.88; H, 7.59; N, 2.23.

***N,N*-Dimethyl-*N*-(2-acetylbenzo[*b*]furan)-*N*-(2-methacryloylethyl)ammonium Triphenylbutyl borate (4b)**. As in the procedure described for **4a**; 42% yield, mp 113−115. ^{1}H NMR (CD_3CN, δ): 7.94 (m, 2H), 7.78 (m, 2H), 7.56 (m, 1H), 7.41 (br s, 6H, ortho to B), 7.09 (t, $J = 7.4$ Hz, 6H, meta to B), 6.96 (t, $J = 7.4$ Hz, 3H, para to B), 6.07 (s, 1H), 5.62 (s, 1H), 4.99 (s, 2H), 4.66 (m, 2H), 4.09 (m, 2H), 3.45 (d, $J = 6.2$ Hz, 6H), 2.29 (t, $J = 7.0$ Hz, 2H), 1.93 (s, 3H), 1.35 (m, 2H), 1.04 (m, 2H), 0.91 (t, $J = 7.0$ Hz, 3H). Anal. Calcd for $C_{40}H_{46}BNO_4$: C,78.09; H, 7.48; N, 2.28. Found: C, 79.12; H, 7.46; N, 2.28.

***N,N*-Dimethyl-*N*-(2-acetylnaphthone)-*N*-(2-methacryloylethyl)ammonium Tetrafluoroborate (5a)**. To a solution of **6a** (1.25 g, 3.08 mmol) in 80 mL of water was added fluoroboric acid (0.62 mL, 4.65 mmol), 48 wt % solution in water at room temperature. After 30 min stirring, solid suspension was filtered and washed with water several times. The solid product was recrystallized from ethanol as white crystals (0.88 g, 70%); mp 129−130 °C. ^{1}H NMR (CD_3CN, δ) 8.70 (s, 1H), 8.15 (m, 4H), 7.83 (m, 2H), 6.0 (s, 2H), 5.54 (s, 1H), 5.28 (s, 2H), 4.70 (m, 2H), 4.23 (m, 2H), 3.53 (s, 6H), 1.87 (s, 3H). Anal. Calcd for $C_{20}H_{24}BF_4NO_3$: C, 58.16; H, 5.81; N, 3.39. Found: C, 58.32; H, 5.78; N, 3.40.

***N,N*-Dimethyl-*N*-(2-acetylbenzo[*b*]furan)-*N*-(2-methacryloylethyl)ammonium Tetrafluoroborate (5b)**. As in the procedure described for **5a** above, **6b** (0.90 g, 2.27 mmol) in 70 mL of water was allowed to react with 48 wt % aqueous fluoroboric acid (0.60 mL, 4.54 mmol), followed by recrystallization from ethanol affords **5b** (0.63 g, 69%) as white solid; mp 157−158 °C. ^{1}H NMR (CD_3CN, δ) 7.94 (m, 2H), 7.78 (m, 2H), 7.55 (m, 1H), 6.06 (s, 1H), 5.60 (s, 1H), 5.08 (s, 2H), 4.68 (m, 2H), 4.16 (m, 2H), 3.51 (s, 6H), 1.92 (s, 3H). ^{13}C NMR (CD_3CN, δ): 181.58, 167.06, 156.69, 150.85, 136.45, 130.77, 127.52, 126.95, 125.62, 125.10, 116.87, 113.18, 65.83, 64.48, 59.17, 54.11, 18.15. Anal. Calcd for $C_{18}H_{22}BF_4NO_4$: C, 53.64; H, 5.46; N, 3.47. Found: C, 53.44; H, 5.51; N, 3.43.

Free-Radical Polymerization of 3a. A solution of **3a** (1.14 g, 1.76 mmol) and 2,2′-azobis(isobutyronitrile) (AIBN, 14 mg, 5 mol %) in dry acetonitrile (16 mL) was charged into an oven-

Scheme 1

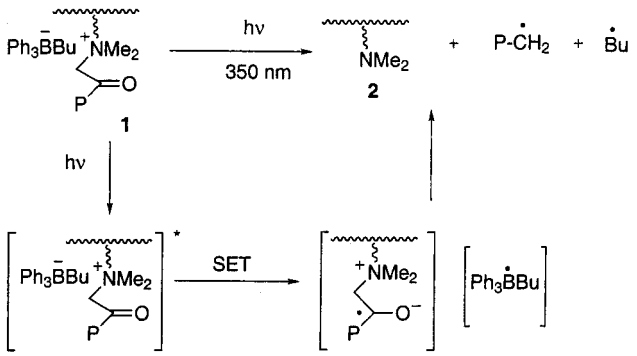

dried polymerization tube. The polymerization tube was subjected to four freeze−pump−thaw cycles, sealed, and heated at 60 °C for 72 h. Insoluble materials were filtered, and the filtrate was poured dropwise with stirring into 200 mL of methanol. The precipitation was collected by filtration and purified by reprecipitation from methanol. After drying in vacuo, **7a** was obtained as white powder (0.65 g, 58%). FTIR (film on NaCl): 3053, 3036, 2984, 1730, 1688, 1625, 1578, 1452, 1426, 1179, 1126, 916, 857, 735, 706, 607. Anal. Calcd for $C_{44}H_{44}BNO_3$: C, 81.90; H, 6.82; N, 2.17. Found: C, 81.38; H, 6.76; N, 2.21.

Polymer 7b. As in the procedure described for **3a**, monomer **3b** (1.32 g, 2.08 mmol) and AIBN (15 mg, 5 mol %) in acetonitrile (12 mL) was heated at 60 °C for 72 h. A yellowish clear solution was filtered, concentrated, and poured into methanol (200 mL). The polymer was purified by dissolving in acetonitrile and then precipitated from methanol again. After drying, polymer **7b** was obtained as a solid (0.90 g, 68%). FTIR (film on NaCl): 3054, 3036, 2999, 1734, 1690, 1611, 1554, 1478, 1427, 1163, 1138, 875, 735, 707. Anal. Calcd for $C_{42}H_{42}BNO_4$: C, 79.41; H, 6.61; N, 2.20. Found: C, 78.98; H, 6.71; N, 2.20.

Polymer 8a. As described before; 90% yield. ^{1}H NMR shows no vinylic protons. FTIR (film on NaCl): 3053, 2951, 2916, 2844, 1731, 1690, 1625, 1595, 1476, 1387, 1276, 1142, 918. Anal. Calcd for $C_{42}H_{48}BNO_3$: C, 80.68; H, 7.68; N, 2.24. Found: C, 80.19; H, 7.58.

Polymer 8b. As described above; 46% yield. FTIR (film on NaCl): 3052, 2951, 2916, 2844, 2795, 1736, 1691, 1599, 1561, 1478, 1443, 1163, 1138, 907, 875, 741, 707. Anal. Calcd for $C_{40}H_{46}BNO_4$: C, 78.09; H, 7.48; N, 2.28. Found: C, 77.68; H, 7.43.

Polymer 9a. As described above; 70% yield. ^{13}C NMR (CD_3CN, δ): 191.68, 177.47, 137.18, 133.25, 132.56, 132.01, 131.05, 130.14, 129.10, 123.97, 67.59, 64.30, 59.82, 53.84, 46.19, 20.61. FTIR (film on NaCl): 3059, 2994, 1730, 1692, 1596, 1482, 1388, 1227, 1182, 1060, 862, 722.

Polymer 9b. As described above; 78% yield. ^{13}C NMR (CD_3CN, δ): 181.85, 177.81, 156.92, 150.92, 131.25, 127.70, 125.95, 125.59, 117.89, 113.52, 66.45, 64.77, 59.90, 53.98, 46.10, 19.52. FTIR (film on NaCl): 3119, 3060, 2991, 1730, 1692, 1612, 1555, 1477, 1291, 1171, 1142, 1056, 948, 876, 756.

Results

Design and Synthesis. In designing our polymeric systems, we chose to incorporate the chromophore acceptors covalently tethered to amine functionality through a spacer $-CH_2-$ and block the tertiary amine groups (Scheme 1). The neutral nitrogen atom of the amine becomes a quaternary nitrogen atom and forms a salt with the electron donor borate (*n*-butyltriphenyl or tetraphenyl) anions. Since the donors and acceptors are contained on the same pendent chain and electron transfer can be assumed to be primarily intramolecular, the quenching will be more efficient.

Scheme 2

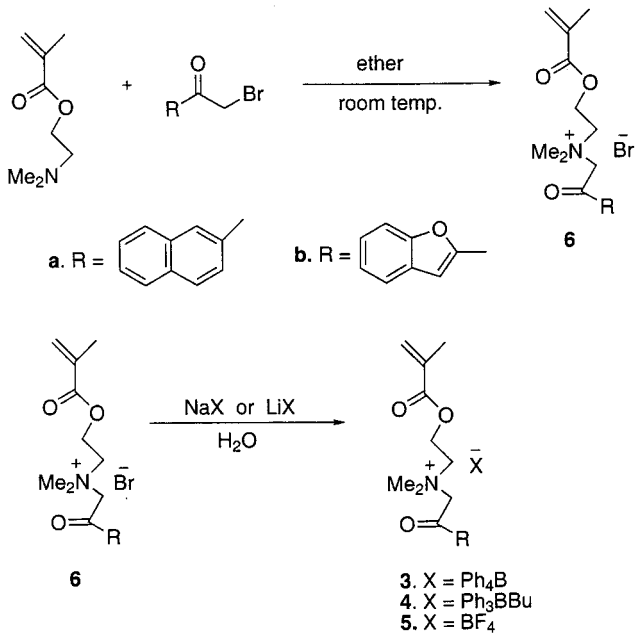

Light is absorbed by chromophore P, and excited states thereby formed oxidize the proximate borate, creating the radical ion pair. Neutral amine and reactive radicals are next released from the radical ion pair by carbon−nitrogen and carbon−boron bond scission, respectively. In this manner, photoreactive polymer **1** generates polymeric amine **2** as well as radicals upon irradiation. In this strategy, one decouples the light absorption step from the amine release or bond scission steps. For this reason, the light-absorbing properties of P can be separately optimized with the mechanism for release of the amine remaining the same. The chromophore itself does not become intimately involved in the release of amine. The choice of chromophore and borate will determine the driving force for electron-transfer reaction[20,21] and subsequent polymeric amine formation from precursors.

Monomers **3**−**5** were made via a straightforward synthesis with good yields (Scheme 2). Bromoacetyl compounds[19] afforded ammonium bromide salts **6** by reaction with the amine functionality of 2-(dimethylamino)ethyl methacrylate. Characterization of the salts by spectroscopic methods indicates that amine protection proceeds in quantitative yield. Reaction of **6** with the corresponding borate salts in water led to the desired monomers, and these were shown to be analytically pure. All were further recrystallized from appropriate solvents before use in radical polymerization.

The method of polymerization is similar for all monomers used and is performed under similar conditions. Radical polymerization of monomers **3**−**5** was carried out in sealed tubes using AIBN [2,2′-azobis(isobutyronitrile)] as radical source at 60 °C in dry inhibitor free acetonitrile (Scheme 3). Purification was accomplished after several precipitations with methanol. Polymers **9a,b** (tetrafluoroborate as counterion) were synthesized as controls where no electron transfer would be expected. All the polymers were highly soluble in acetonitrile, acetone, and DMF but insoluble in toluene, ether, THF, methanol, and ethanol.

Characterization. Structures were established via FTIR, ^{1}H NMR, and elemental analysis. Most of the peaks in the ^{1}H NMR spectra were broadened due to

Scheme 3

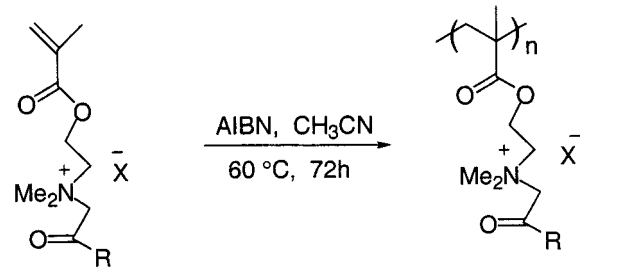

3. X = Ph_4B
4. X = Ph_3BBu
5. X = BF_4

7. X = Ph_4B
8. X = Ph_3BBu
9. X = BF_4

Table 1. Thermal Properties of Polymers

polymer	% yield	T_m (°C)	T_d (°C)
7a	58	153	202
7b	67	112	168
8a	90	122	174
8b	52	109	160

the long as well as bulky side chains attached to the polymer backbone. However, resonances due to the vinylic moiety in the polymer in the 6.5−5.4 ppm region were absent. These results indicate no residual monomer is present in final polymers. Additional information about the structure of the polymers comes from FTIR spectra. The disappearance of acrylate bands 811 cm^{-1} in the FTIR spectrum of the polymers indicates a high degree of polymerization occurs under the experimental conditions. However, IR absorptions at 1730 cm^{-1} due to ester groups of the methacrylate moieties and at 1680−1690 cm^{-1} due to the carbonyl group adjacent to the chromophores were obvious.

Molecular weight determination by gel permeation chromatography (GPC) was not possible using our existing system with THF eluent due to the highly ionic nature of the polymers. However, each of the polymers forms a smooth film from a solution in acetonitrile or DMF, indicating that the molecular weights of all polymers are quite high.

Thermal Properties. Neither polymer **7** nor **8** showed any glass transition, T_g, upon DSC analysis, in agreement with the assumed highly crystalline properties due to the ionic nature of the polymers. However, DSC did show melting points for all the polymers. Thermal stabilities were determined in nitrogen by thermal gravimetric analysis (TGA) (Table 1). TGA measurements of all showed a clean two-step degradation curve, and the thermal stability limit, T_d, was taken as the temperature at which 5% weight loss of a sample occurred. It varied from 160 to 202 °C. The first step corresponding to a weight loss of 48−50% matched well with the loss of tetraorganoyl borates. Significant weight loss was also detected at 300−420 °C, the onset temperature for the second step, indicating the decomposition of the remaining products.

Photophysical Properties. The absorption spectra of **8a** and **8b** in acetonitrile are shown in Figure 1. The spectrum for **8a** clearly shows the low-energy n−π^* transition at 348 nm ($\log \epsilon = 3.35$) corresponding to the S_1 state followed by an intense band due to the electric dipole allowed π−π^* transition at 300 nm corresponding to the S_2 state. The spectrum of **8b** has one broad peak at 308 nm ($\log \epsilon = 4.36$), and no sharp n−π^* transitions were observed because these are hidden under the strong π−π^* transition band.

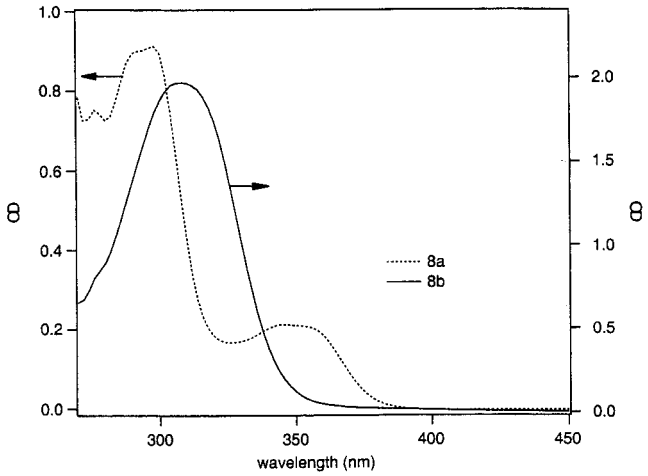

Figure 1. UV absorption spectra of polymer **8a** and **8b** in acetonitrile.

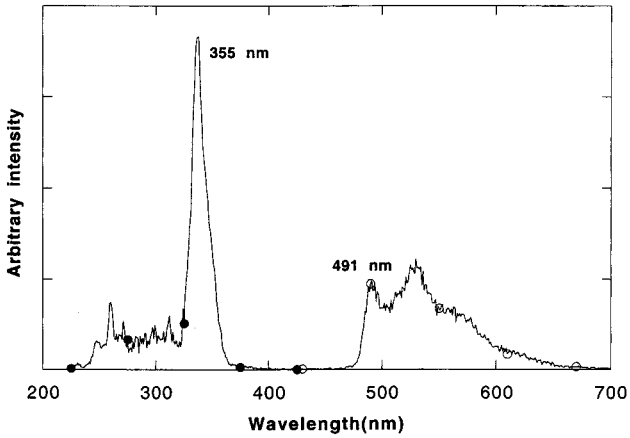

Figure 2. Phosphorescence emission and excitation spectra of **9a** in EPA.

Table 2. Phosphorescence Data for 9a and 9b in EPA

polymer	λ_{max} (nm)	E_T (kcal/mol)	τ_p (s)	Φ_p
9a	488, 526	58.8	1.10	3.9×10^{-4}
9b	490, 526	58.3	0.08	3.1×10^{-3}

The absorption maxima are red-shifted upon changing the solvent from acetonitrile to benzene, and the absorption characteristics of each of the polymers depend on the chromophore, not on the structure of the anions. Polymers **9a** and **9b** (nonoxidizable counterion BF_4^-) fluoresce in acetonitrile with quite low quantum yields, indicating a rapid depopulation of the singlet excited states by intersystem crossing (ISC). This is corroborated by phosphorescence measurements. No fluorescence quenching was observed upon the addition of borate donors such as Ph_4B^-,$^+NBu_4$ or Ph_3BuB^-,$^+NBu_4$. Figure 2 shows the phosphorescence spectrum of **9a** in EPA (ether:isopentane:ethanol = 5:5:2) at 77 K. The broad phosphorescence emission observed is usually associated with a π−π^* triplet electronic configuration. The relevant data of phosphorescence of **9a,b** were tabulated in Table 2.

An interesting spectroscopic feature is a large red shift between the absorption spectrum and the phosphorescence excitation spectrum for **9b** (38 nm). This occurs due to the participation of two different excited singlet states in this particular photoprocess. The symmetry-forbidden S_1 state (excitation maximum) populates the emitting triplet state T_1 more efficiently than

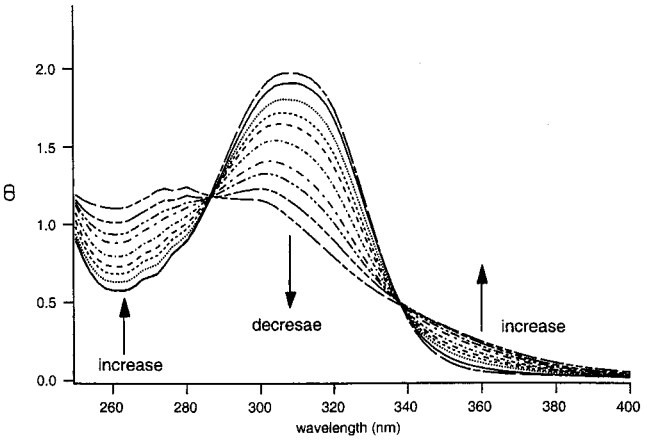

Figure 3. Irradiation of **8b** at different irradiation times with a light intensity of 9.23×10^{-10} E/s (irradiation times in s for the spectra from top to the bottom: 1 = 0; 2 = 99; 3 = 297; 4 = 494; 5 = 890; 6 = 1484; 7 = 2375; 8 = 3665; 9 = 4565; 10 = 7265).

the allowed S_2 state (absorption maximum). Therefore, it is a logical assumption that the internal conversion (IC) from S_2 to S_1 is relatively slow compared to ISC from S_1 to T_1.

Polymer Photolysis: Characterization of Photoproducts. Photolysis of polymer **9a** or **9b** in acetonitrile (Rayonet reactor, λ = 350 nm) produced no detectable products whereas under similar conditions, polymers **7a,b** and **8a,b** produce a yellowish color upon irradiation. Figure 3 shows the absorption spectra of **8b** as a function of irradiation time.. Two isosbestic points at 298 and 338 nm were observed, indicating that polymer photodegradations proceeded selectively without side reaction.

Since the spectra of the irradiated solutions consist of broad, shapeless peaks, ^{1}H NMR analysis is of only limited value. Nonetheless, the formation of polymeric amine by C−N bond cleavage was determined by observing the appearance of sharp peaks around 2.45 ppm due to dimethylamino pendent group. An irradiation time of less than 1 h was found to be sufficient for 100% conversion into polymeric amines.

Table 3. Quantum Yields for Decomposition of Compounds 7 and 8 in Acetonitrile

compound	Φ_d (aerobic)	Φ_d (anaerobic)
7a	0.08	0.15
8a	0.20	0.24
7b	0.18	0.23
8b	0.31	0.54

Polymers were irradiated in acetonitrile for 1 h and subjected to GC-MS analysis. Scheme 4 shows the photoproducts after photolysis at 350 nm. Similar photoproducts are also found from **7b** and **8b**. This supports a general mechanism for the photodegradation process.

Products **11**−**13**, despite their variety, all derive from radical **16**. The benzofuran chromophore derivatives also show similar products, indicating the formation of radical **17**. Product **11** is the result of dimerization of **16** while compound **13** forms by hydrogen abstraction from solvent. Compound **12** is the cross-coupling product formed from **16** and a butyl radical. Formation of the butyl radical, which occurs due to C−B bond cleavage, is also confirmed by the appearance of octane **14**. In the case of compounds that contain the Ph_4B^- anion, both C−N and C−B bond cleavage occur as well. However, the phenyl radical does not couple with radical **16** or **17**. Instead, it abstracts hydrogen from the solvent at a diffusion-controlled rate.[22] The presence of phenyl radical is also confirmed by radical trapping experiments with methyl methacrylate.[23] The chemistry of biphenyl **15** formation is complex. The mechanism of the formation of biphenyl involves rearrangement reactions of boron derivatives.[24]

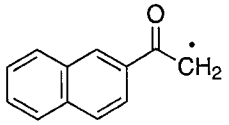

16

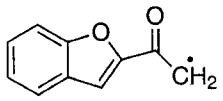

17

Quantum yields for the photodegradation of **7a**, **7b**, **8a**, and **8b** are shown in Table 3. These data clearly show the influence of oxygen, as well as the effect of

Scheme 4

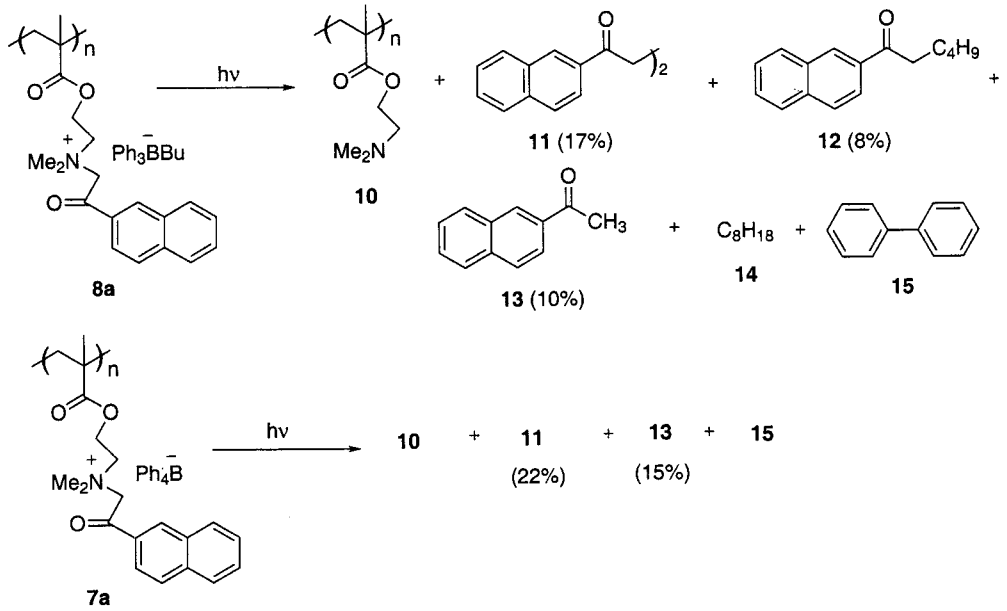

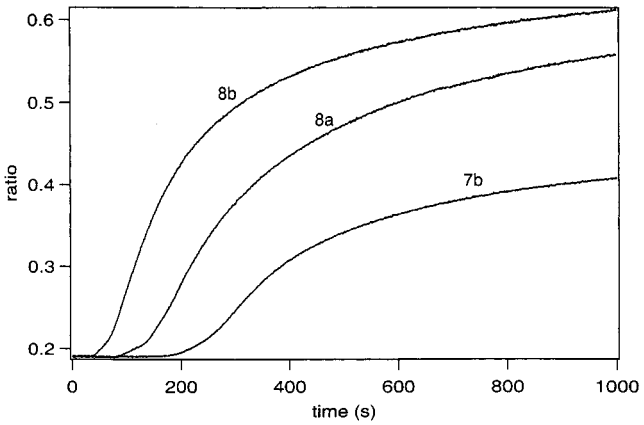

Figure 4. Cure monitor profiles (ratio of fluorescence at 456 and 558 nm) for photopolymerization of TEGDA using the polymeric photoinitiators **7b**, **8a**, and **8b** (OD: **8a** = 0.097, **8b** = 0.094, **7b** = 0.062).

the structure of the acceptor and donor (borate) on the photodegradation process.

Polymerization Efficiency. The efficiency of the polymers as initiators in polymerization reactions was measured by recording the initiated polymerization profile in TEGDA under steady-state conditions using the fluorescence cure monitor.[8] Kinetics were followed using fluorescence probe methodology,[16] and the relative efficiencies η_i of the initiators were calculated in representative monomers using a protocol previously described (Figure 4).[8] A more quantitative indication of initiator efficiency can be obtained from the inhibition time[11,25,26] t_i when polymerization starts and mass transfer in the cross-linking system is, thus, of less importance. In general, this treatment is valid as long as oxygen can be considered as the main inhibiting species.

One can obtain the initiator efficiency, which is a product of Φ_d and the radical yield factor f,[27] using eq 1.

$$\eta_i = \Phi_d f = C\frac{1}{t_i}\frac{1}{I_0}\frac{1}{(1-10^{-OD})} \qquad (1)$$

Substituting the values for t_i, the light intensity I_o, and the optical density of the initiator OD one can easily obtain the relative efficiency. C is a constant that contains the rate constants for initiation and termination by oxygen. However, since we used commercial Irgacure 651 as a reference initiator, the specific values for C are not necessary because the efficiencies obtained are relative values. The relative efficiencies of **7b**, **8a**, and **8b** were found to be 0.21, 0.16, and 0.50, respectively. **7a** was too insoluble, and its efficiency could not be determined under our experimental conditions. Overall, polymers containing the acetobenzo[*b*]furan chromophore **8a,b** are better initiators than the chromophore acetonaphthone. As will be discussed latter, the efficiency is also related to the oxidation potentials of borate donors. Polymer **8b**, which has the triphenylbutylborate anion, can initiate polymerization much faster than **8a** (containing tetraphenylborate).

Discussion

Product analysis indicates that both the carbon−nitrogen and carbon−boron bonds cleave during the photolysis in acetonitrile. Polymers **9a** and **9b**, which contain only the acceptor moiety, show no detectable products upon photolysis. This says that the primary step leading to cleavage is electron transfer from the borate anion to excited acceptors. Model studies[18] have shown that the driving force, $\Delta G°$, for **7** and **8** is highly negative in acetonitrile, indicating the feasibility of electron-transfer reaction. The involvement of the triplet state was suggested by observing spectroscopic quenching with the borates. The mechanism for photocleavage appears to be general (Scheme 5).

Scheme 5

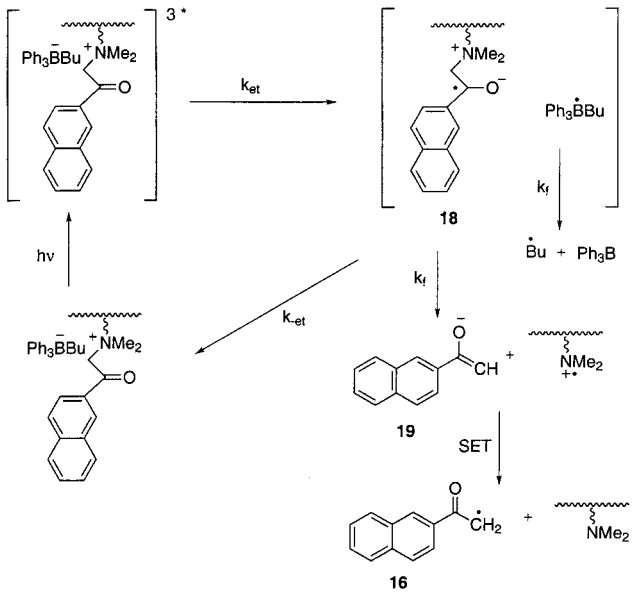

The triplet radical pair **18** was generated after the electron transfer. Once formed, the carbon-centered radical undergoes rearrangement, followed by fragmentation of carbon−nitrogen bond, yielding anion **19**. Homolytic dissociation of the carbon−nitrogen bond is not unlikely because of the low electronegativity difference between the carbon and nitrogen atom.[28] The possibility of heterolytic carbon−nitrogen bond cleavage is ruled out, since this does not lead to formation of the radicals **16**, which were shown to be formed. In radical pair **18**, on the other hand, boronyl radicals decompose to butyl or aryl radicals (in the case of Ph_4B), and these are believed to be the initiating species in polymerization reactions. Both oxidative and reductive decompositions take place fast (pico- or subpicosecond time scale)[10] so the back electron transfer cannot compete. Back electron transfer is also a spin-forbidden process in the triplet states.[29] Irrespective of the chromophores and anions, the quantum yields of the photodecompositions were found to be more than 0.10 in the absence of oxygen. In this respect, the bulky tributylammonium group on nitrogen plays an important role in that it provides effective hyperconjugative interaction of the carbon−nitrogen bond with the excited π-system of the acceptor, thus making for an effective dissociation.[28]

Quantum yields are found lower for polymeric systems than for their small molecule analogues. The influence of oxygen becomes a minor factor in cross-linking in radical bulk polymerizations since this occurs faster than diffusion of dissolved oxygen through the monomer to the irradiated reaction center. However, there seems to be little relationship between the quantum yields of decomposition and the efficiencies of the polymers as initiators since the quantum yields were

conducted in the solvent acetonitrile while photopolymerization requires the experiments be carried out in bulk monomer. Furthermore, the photoinitiators produce two types of initiating species (butyl and phenyl radical) from the borates, and these have different reactivities in radical polymerization.

Efficiency increases with an increase of the acceptor strength of the chromophore (half-wave reduction potential) and the electron-donating property of the borate (half-wave oxidation potential). The efficiency of **8b** is higher than that of **8a** (due to reduction potentials of chromophore), and similarly, the efficiency of **8b** is higher than that of **7b** (due to oxidation potential of borate).[30] These results again are consistent with the photocleavage electron-transfer mechanism. In conclusion, these polymeric systems are stable compared to small molecule analogues and most conventional small molecule photoinitiators. Further opportunities for their use are being explored.

Acknowledgment. This work has been supported by the National Science Foundation (NSF 9526755) and the Office of Naval Research (N00014-97-1-0834). The authors are most grateful for this support.

References and Notes

(1) Contribution No. 382 from the Center for Photochemical Sciences.
(2) Carlini, C.; Angiolini, L. *Advances in Polymer Sciences*; Springer: Berlin, 1995; Vol. 123, p 127.
(3) Davidson, R. S. *J. Photochem. Photobiol. A: Chem*. **1993**, *69*, 263.
(4) Allen, N. S. *J. Photochem. Photobiol. A: Chem*. **1996**, *100*, 101.
(5) Hassoon, S.; Sarker, A.; Polykarpov, A. Y.; Rodgers, M. A. J.; Neckers, D. C. *J. Phys. Chem*. **1996**, *100*, 12386.
(6) Sarker, A. M.; Lungu, A.; Neckers, D. C. *Macromolecules* **1996**, *29*, 8027.
(7) Sarker, A. M.; Kaneko, Y.; Nikolaitchik, A. V.; Neckers, D. C. *J. Phys. Chem*. **1998**, *102*, 5375.
(8) Popielarz, R.; Sarker, A. M.; Neckers, D. C. *Macromolecules* **1998**, *31*, 951.
(9) Hu, S.; Sarker, A. M.; Kaneko, Y.; Neckers, D. C. *Macromolecules* **1998**, *31*, 6476.
(10) Sarker, A. M.; Kaneko, Y.; Neckers, D. C. *J. Photochem. Photobiol. A: Chem*. **1998**, *117*, 67.
(11) Strehmel, B.; Sarker, A. M.; Malpert, J. H.; Neckers, D. C. *Polym. Prepr*. **1998**, *39* (2), 725.
(12) Chatterjee, S.; Gottschalk, P.; Davis, P. D.; Schuster, G. B. *J. Am. Chem. Soc*. **1988**, *110*, 2326.
(13) Chatterjee, S.; Davis, P. D.; Gottschalk, P.; Kurtz, M. E.; Sauerwien, B.; Yang, X.; Schuster, G. B. *J. Am. Chem. Soc*. **1990**, *112*, 6329.
(14) Schuster, G. B. *Pure Appl. Chem*. **1990**, *62*, 1565.
(15) Davidson, R. S. In *Radiation Curing in Polymer Science and Technology;* Fouassier, J. P., Rabek, J. F., Eds.; Elsevier-Applied Science: Essex, U.K., 1993; Vol. 111, p 153.
(16) Neckers, D. C.; Song, J. C.; Torres-Filho, A.; Jager, W. F.; Wang, Z. J. U.S. Patent 5,606,171, 1997.
(17) Niizuma, K.; Koizumi, M. *Bull. Chem. Soc. Jpn*. **1963**, *36*, 1629.
(18) Kaneko, Y.; Sarker, A. M.; Neckers, D. C.*Chem. Mater*. **1999**, *11*, 170.
(19) Sarker, A. M.; Neckers, D. C., unpublished results.
(20) Fox, M. A., Chanon, M., Eds. *Photoinduced Electron-Transfer Reactions*; Elsevier: Amsterdam, 1988.
(21) Kavarnos, G. J.; Turro, N. J. *Chem. Rev*. **1986**, *86*, 401.
(22) Kryger, R. G.; Lorand, J. P.; Stevens, N. R.; Herron, N. R. *J. Am. Chem. Soc*. **1977**, *99*, 7589.
(23) Sarker, A. M.; Kaneko, Y.; Neckers, D. C. *J. Photochem. Photobiol. A: Chem*. **1999**, *121*, 83.
(24) Bancroft, E. E.; Blount, H. N.; Janzen, E. G. *J. Am. Chem. Soc*. **1979**, *101*, 3692.
(25) Moad, G.; Salomon, D. H. *The Chemistry of Free Radical Polymerization*; Pergamon Press: New York, 1995.
(26) Müller, U. *J. Macromol. Sci., Pure Appl. Chem*. **1994**, *A31*, 1905.
(27) The initiation efficiency *f* is defined by the ratio of radicals escaped from solvent cage to form initiating radicals to the overall number of produced radicals.[25]
(28) Michl, J. *Acc. Chem. Res*. **1990**, *23*, 127.
(29) Ci, X.; da Silva, R. S.; Nicodem, D. E.; Whitten, D. G. *J. Am. Chem. Soc*. **1989**, *111*, 1337.
(30) Reduction potentials for acetonaphthone and acetobenzo[*b*]-furan are −1.27 V vs SCE and −1.32 V vs SCE, respectively.[9] Similarly, oxidation potentials for tetraphenylborate and triphenylbutylborate are 0.90 and 0.70 V, respectively.[18]

MA990127C